Kinetics on Formation of Hyperbranched Poly(ethyl methacrylate) via a Controlled Radical Mechanism of Photofunctional Inimer

Koji Ishizu,* Takeshi Shibuya, and Susumu Kawauchi

Department of Organic Materials and Macromolecules, International Research Center of Macromolecular Science, Tokyo Institute of Technology, 2-12-1, Ookayama, Meguro-ku, Tokyo 152-8552, Japan

Received December 2, 2002; Revised Manuscript Received February 28, 2003

ABSTRACT: We studied the living nature on the formation of hyperbranched poly(methacrylic acid ester) by free radical photopolymerization of 2-(*N*,*N*-diethyldithiocarbamyl)ethyl methacrylate (DTEM) in benzene. We performed the first-order time−conversion plots in this polymerization system, and the straight line in the semilogarithmic coordinates indicated that the polymerization is first order in monomer. The number-average molecular weight (M_n) of hyperbranched polymers increased with increasing conversion. The free radical polymerization proceeded with controlled radical mechanism. Subsequently, we treated the kinetics of initiation and propagation steps of the active A* and B* (side group) sites using model compounds. The degradation rates of two types of dithiocarbamate (DC) groups at A and B sites agreed well with theoretical trends in C−S bond dissociation energies predicted by the density functional theory for model compounds. The reactivity of the initiating B* was less than that of propagating A* groups. The degree of branching of hyperbranched polymers was discussed using both reaction rates.

Introduction

Highly branched topologies have become a major research interest in polymer science.[1,2] Recent advances in living polymerization have allowed facile preparation of hyperbranched polymers. Self-condensing vinyl polymerization was first demonstrated using a living cationic polymerization[3] and later expanded to 2,2,6,6-tetramethylpiperidinyloxy (TEMPO)-mediated living radical[4] and group-transfer polymerization processes.[5,6] Atom transfer radical polymerization (ATRP) of *p*-chloromethylstyrene similarly provided hyperbranched polymers.[7,8] Controlled radical polymerization initiated by nitroxide and nitroxyl compounds also provided the hyperbranched polymers.[9−11]

More recently, we presented novel routes to hyperbranched polymers from (*N*,*N*-diethyldithiocarbamyl)-methylstyrene (DTCS)[12] and 2-(*N*,*N*-diethyldithiocarbamyl)ethyl methacrylate (DTEM; **1**)[13] as inimers by a one-pot photopolymerization. DTCS or DTEM was capable of initiating living radical polymerization of the vinyl group. Subsequently, hyperbranched polystyrenes (PS) were prepared by photo-copolymerization of DTCS with styrene.[14] DTCS and styrene had equal reactivity toward both propagating species, and the copolymer composition was the same as the comonomer feed. These radical mechanisms were very similar to alkoxyamine-initiated living radical polymerization system established by Moad and Rizzardo.[15] To understand the reaction process of such self-addition vinyl polymerizations, it is necessary to analyze the kinetics of these reactions.

Recently, Müller and co-workers[16] calculated the molecular parameters of hyperbranched PSs formed by self-condensing vinyl polymerization of *p*-chloromethylstyrene (CMS) inimer with the general structure AB*, where A is a vinyl group and B* is an initiating group. Our photopolymerization systems also proceed with almost similar mechanism described above. In a previous paper,[17] we reported the kinetics of hyperbranched PSs by free radical polymerization of photofunctional inimer DTCS. The first-order time−conversion plots in polymerization of inimer DTCS fit well on a straight line. We concluded that free radical polymerization of inimer DTCS proceeded with a controlled radical mechanism. We also plotted the semilogarithmic relationship of weight-average molecular weight (M_w) against conversion. The observed values of M_w fit well on a straight line in the semilogarithmic plot.

DTEM also provides hyperbranched poly(methacrylic acid ester) by a similar radical mechanism. Initiation occurs by addition of the active B* group to the double bond of another monomer (see Scheme 1). Photolysis of **1** produces initiating methacryloyl ethyl radical and a less reactive dithiocarbamate (DC) radical.[18−20] The dimer **2** formed has two DC active sites and one double bond. Both the initiating B* group and the newly created propagating center, A*, can react with the vinyl group of any other molecule (inimer or polymer) in the same way with rate constant k_p^A and k_p^B, respectively. The initial steps up to the formation of trimers **3** are shown in Scheme 1. The addition of a vinyl group to a terminal A* or B* center leads to a linear linkage, whereas the addition of a double bond to a side group B* (**3b**) or an A* center within the polymer (center of **3a**) leads to a branch point.

In this article, we studied the living nature on the formation of hyperbranched poly(methacrylic acid ester)s by free radical polymerization of photofunctional inimer **1** and studied the kinetics of initiation and propagation of the active A* and B* sites using model compounds. We also demonstrated that density functional theory calculations reliably and quantitatively predict the experimentally observed trends in C−S bond dissociation energies for several model compounds. The degree of branching (DB) was discussed using both propagation rates.

* Corresponding author: Fax +81-3-5734-2888; e-mail kishizu@polymer.titech.ac.jp.

10.1021/ma021729q CCC: $25.00
Published on Web 04/18/2003

Scheme 1

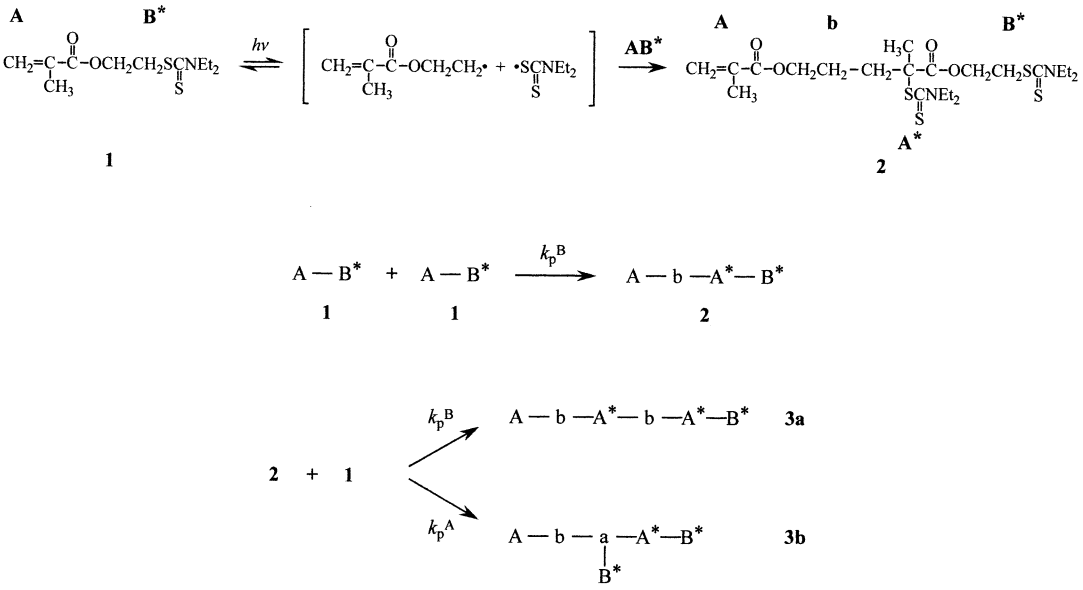

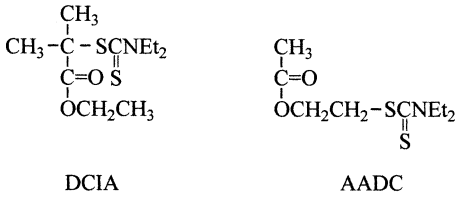

DCIA AADC

Figure 1. Chemical structures of model compounds DCIA and AADC.

Experimental Section

Materials. 2-Chloroethyl methacrylate (Lancaster, UK) and ethyl methacrylate (EMA: Tokyo Kasei Organic Chemicals) were distilled in high vacuum. Ethyl 2-bromoisobutyrate, 2-chloroethyl acetate (Tokyo Kasei Organic Chemicals; >98%), *N*,*N*-diethyldithiocarbamate sodium salt (Kanto Chemicals; >98%), and TEMPO free radical (Aldrich; 99%) were used as received.

Synthesis of Inimer and Model Compounds. Inimer DTEM was synthesized by the reaction of 2-chloroethyl methacrylate with *N*,*N*-diethyldithiocarbamate sodium salt in acetone.[13] To a solution of 2-chloroethyl methacrylate (0.1 mol) in acetone (100 mL) was added *N*,*N*-diethyldithiocarbamate sodium salt (0.12 mol), and the reaction mixture was stirred at 40 °C. The precipitated NaCl salt was removed by filtration. Acetone was evaporated from the reaction mixture. The crude mixture was dissolved in benzene, and insoluble *N*,*N*-diethyldithiocarbamate sodium salt was removed by filtration. The benzene solution was washed with water, and the organic extract was evaporated to dryness. The crude product was purified by silica column chromatography, eluting with 3:1 dichloromethane/hexane to give DTEM as colouless oil. Yield 95%. ^{1}H NMR ($CDCl_3$) δ: 1.30 ppm (6H, $-CH_3$; methyl protons of DC group), 1.97 (3H, $-CH_3$), 3.70 and 4.39 (4H, $-CH_2-$ of DC group), 5.61 and 6.14 (2H, $=CH_2$).

Two model compounds 2-(*N*,*N*-diethyldithiocarbamyl)isobutyric acid ethyl ester (DCIA) and acetic acid 2-(*N*,*N*-diethyldithiocarbamyl)ethyl ether (AADC) were also synthesized by a similar reaction using ethyl 2-bromoisobutyrate and 2-chloroethyl acetate, respectively (see the chemical structures in Figure 1), to assign the chemical shift of proton signals in NMR. DCIA: Yield 96%. ^{1}H NMR ($CDCl_3$) δ: 1.72 ppm (6H, $-CH_3$), 3.70 and 3.94 (4H, $-CH_2-$ of DC group), 4.20 (2H, $-CH_2-$), and 1.23−1.28 (9H, $-CH_3$ and $-CH_3$ of DC group). AADC: Yield 96%. ^{1}H NMR ($CDCl_3$) δ: 2.06 ppm (3H, $-CH_3$), 3.61 and 4.32 (4H, $-CH_2CH_2-$), 3.76 and 4.03 (4H, $-CH_2-$ of DC group) and 1.28 (6H, $-CH_3$ of DC group).

Photopolymerization. Photopolymerizations of **1** (50 wt % benzene solution) were carried out varying the irradiation time at 40 °C in a sealed glass ampule under high vacuum (250 W high-pressure mercury lamp, Ushio Denki SXUI 250 HAMQ; UV intensity 42 mW/cm^2, irradiation distance 15 cm). After polymerization, the polymer was recovered by evaporating the solvent. We also carried out the photopolymerizations of model compound DCIA as the initiator with ethyl methacrylate (EMA) (50 wt % benzene solution).

Kinetics of Initiation and Propagation Steps. The values of initiation rate R_i were measured by using TEMPO free radical as follows. Free radical polymerization of EMA was carried out in benzene at 40 °C initiated by model compound DCIA or AADC under UV irradiation of TEMPO. The initial time of consumption of the vinyl groups of EMA was measured by dilatometry. That is, the amount of volume shrinkage of polymer produced was measured by height change of the solution through a capillary (ϕ = 2 mm). Densities of EMA monomer and poly(methyl methacrylate) [PMMA; in place of poly(ethyl methacrylate)] are 0.917 and 1.190 g/cm^3 at 20 °C, respectively.[21]

The propagation rate constant k_p^A was estimated by the following method. We performed the first-order time−conversion plot in the photopolymerization of EMA initiated by model compound DCIA. This plot (straight line in the semilogarithmic coordinates) indicates that the polymerization proceeds by a living mechanism. Then, if the concentration of propagating PEMA radical [P_A*] is known value, we can estimate the value of k_p^A from the slope of the first-order plot.

Characterization. A combination of gel permeation chromatography (GPC) with light scattering (LS) detector was used to measure the weight-average molecular weight (M_w) and molecular weight distribution (M_w/M_n) of the hyperbranched molecules. GPC measurements were carried out with a Tosoh high-speed liquid chromatograph HLC-8120 equipped with a low-angle laser light scattering (LALLS) detecor, LS-8 [He−Ne laser (λ_0 = 632.8 nm) with a detection angle of 5°], and refractive index (RI), which was operated with two TSK gel columns, GMH_{XL} [excluded-limit molecular weight (M_{EL} = 4 × 10^8) and $G2000H_{XL}$ (M_{EL} = 1 × 10^4), in series using tetrahydrofuran (THF) as the eluent (flow rate 1.0 mL/min) at 38 °C. The refractive index increment [(d*n*/d*c*) = 0.100 mL/g] of poly(ethyl methacrylate) (PEMA) hyperbranched polymer was determined by a refractometer in THF. The conversion was estimated from the vinyl protons (δ 5.61 and 6.14 ppm) of unreacted inimer **1** in the ^{1}H NMR spectrum of each product (500 MHz, JEOL GSX-500 NMR spectrometer in $CDCl_3$).

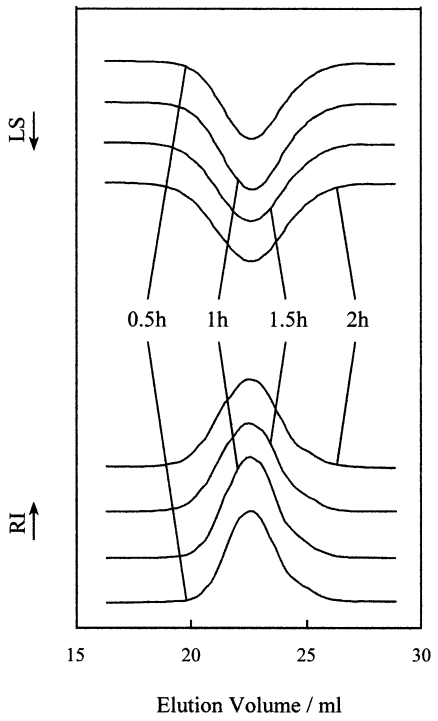

Figure 2. GPC profiles of hyperbranched polymers as a function of irradiation times: GPC measurements were carried out in THF at 38 °C. Photopolymerizations of **1** (50 wt % benzene solution) were carried out at 40 °C: HB1 (irradiation time = 0.5 h), HB2 (1 h), HB3 (1.5 h), and HB4 (2 h) (see in Table 1).

Density Functional Theory Calculations. To understand the observed R_i, we performed density functional theory calculations (B3LYP functional using 6-31G-(d) basis set)[22] for various model compounds DCIA, AADC, inimer **1**, and dimer **2**. These calculations were conducted for a series of carbamates to establish a correction between structure and C−S homolysis rates. C−S bond energies were calculated assuming a homotylic bond cleavage corrected with zero-point energy.

Results and Discussion

Photopolymerizations of **1** were carried out varying the irradiation time. No cross-linked or insoluble materials were observed. GPC profiles for this system showed a unimodal distribution as mentioned in the previous paper[11] and shown in Figure 2. The degree of polymerization (DP_n) increases gradually with increasing reaction times. However, the separation effect of the GPC columns used in this work was poor due to relatively small DP_n of hyperbranched polymers. We will discuss the branched structure using other parameters (a low value of the Mark−Houwink parameter in comparison to that of linear polymer and some hydrodynamic parameters) later. The conversion was estimated from the vinyl protons at 5.61 and 6.14 ppm of unreacted inimer **1** in the ^{1}H NMR spectrum of each product. The M_w and M_w/M_n were determined by GPC-LALLS. The polymerization conditions and results are listed in Table 1.

To better understand the mechanism of propagation, we performed the first-order time−conversion plots in the photopolymerizations HB1−HB4 (see line H in Figure 3), where $[M]_0$ is the initial concentration of inimer **1**. Straight lines in the semilogarithmic coordinates indicate a constant concentration of the active species, which indicates that polymerizations of inimer **1** proceed by a living mechanism, and are first order in monomer. The slope of the semilogarithmic plot, $S_H = R_p^H/[M]$ (where $R_p^H = -d[M]/dt$), was set equal to 2.13 × 10^{-4} s^{-1}. We will discuss this propagation rate R_p^H later.

Table 1. Polymerization Conditions and Results of Hyperbranched Polymers[a]

expt no.	irradiation time (h)	conv[b] (%)	$10^4 M_w$[c]	M_w/M_n[c]	$10^4 M_n$[d]
HB1	0.5	28.5	4.25	1.70	2.50
HB2	1.0	54.8	6.80	1.86	3.66
HB3	1.5	70.0	9.27	2.15	4.31
HB4	2.0	77.5	10.35	2.24	4.62

[a] Photopolymerizations of DTEM (50% benzene solution) were carried out varying the irradiation time at 40 °C. [b] Estimated from vinyl protons at 5.61 and 6.14 ppm of unreacted DTEM by ^{1}H NMR in $CDCl_3$. [c] Determined by GPC-LALLS in THF as eluent at 38 °C. [d] Calculated from the values of M_w and M_w/M_n.

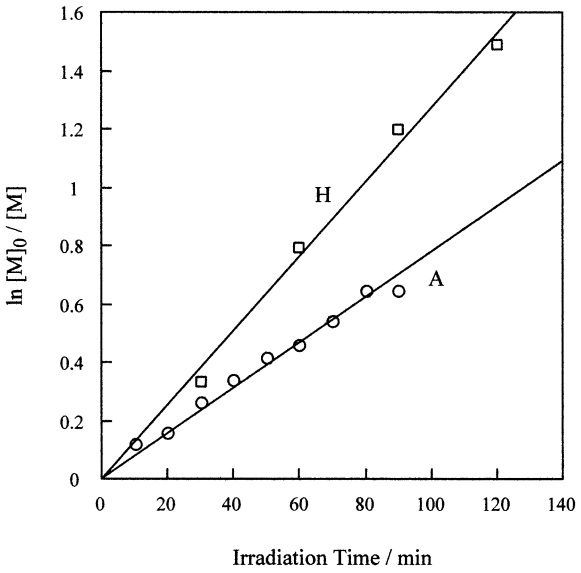

Figure 3. First-order time−conversion plots: line H, polymerization system of inimer DTEM in benzene at 40 °C; line A, polymerization system of EMA (50% benzene solution) initiated by DCIA at 40 °C.

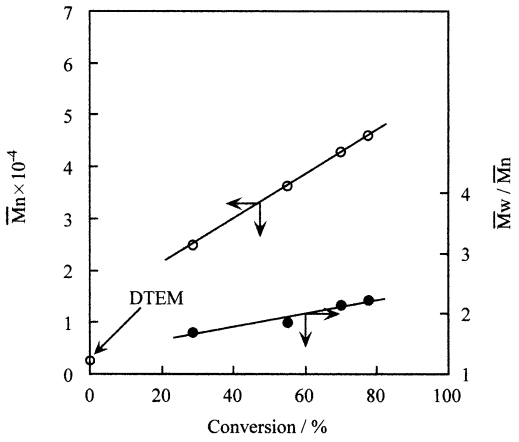

Figure 4. Plot of number-average molecular weight (M_n) or molecular weight distribution (M_w/M_n) against conversion for hyperbranched polymers HB1−HB4.

Figure 4 shows the plot of M_n or M_w/M_n against conversion for such photopolymerization. The observed values of M_n fit well to the straight line beyond ca. 25% of conversion. The intercept is larger than expected value (molecular weight of inimer = 261.41). In the case

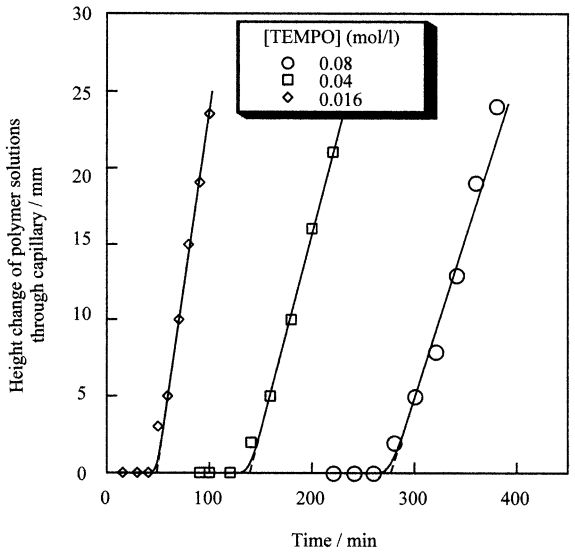

Figure 5. Relationship between volume shrinkage of polymer solutions and induction periods: EMA (3.9 mol/L) was polymerized in benzene at 40 °C initiated by AADC (7.02×10^{-2} mol/L) under UV irradiation using capillary (ϕ = 2 mm), varying the addition amounts of TEMPO (0.016, 0.04, and 0.08 mol/L).

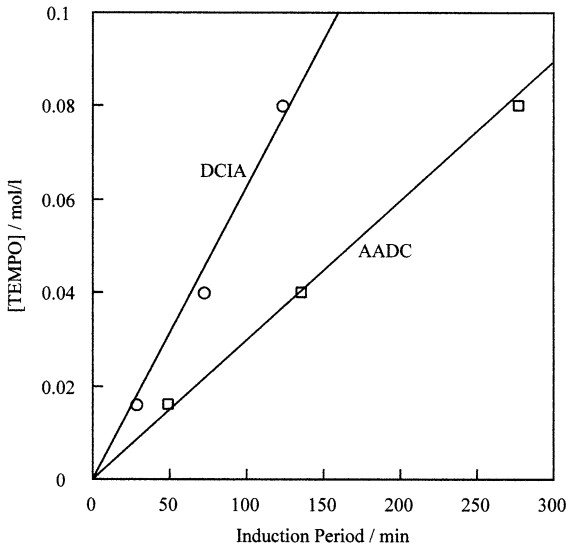

Figure 6. Relationship between feed amounts of TEMPO and induction periods: EMA (3.9 mol/L) was polymerized in benzene at 40 °C initiated by DCIA or AADC (7.02×10^{-2} mol/L) under UV irradiation, varying the addition amounts of TEMPO (0.016, 0.04, and 0.08 mol/L).

that the reactivity changes with size of the macromolecules, the molecule size at which the reaction becomes slower should be identical. This effect is congruent with Fréchet's[3] and Ishizu's[17] observations that the condensation occurs faster in the initial stage. According to Fréchet's explanation,[3] this may be due to a lower accessibility of reactive centers inside larger branched molecules. If that is the case, the kinetic curve of $\ln[M]_0/[M]$ vs time could deviate largely from the linear character at least at the initial stage of polymerization. Further investigation concerning additional data (for example, the absolute value of M_n by vapor pressure osmometer, analysis of branched structure, etc.) between conversion 0−25% is necessary. The polydispersity index is not narrow (M_w/M_n = 1.7−2.4). According to Muller's theoretical calculation,[16] the predicted polydispersity index increased exponentially with conversion (in the case of $k_p^A = k_p^B$ for the formation of hyperbranched polymers). Therefore, this polymerization system seems to proceed with competitive reactions between the initiator radical (ethyl ester-type radical) and the monomer vinyl radical.

To understand the mechanism of hyperbranched polymer formation, we analyzed the reaction steps of initiation and propagation using model compounds. First, the values of R_i were measured using model compounds AADC and DCIA as initiators under following conditions. EMA (3.9 mol/L) was polymerized in benzene initiated by AADC (7.02×10^{-2} mol/L) under UV irradiation, varying the addition amounts of TEMPO (0.016, 0.04, and 0.08 mol/L). Figure 5 shows the relationship between the induction period and height changes of the solution through a capillary. The relationship of these induction periods and feed of TEMPO is shown in Figure 6 (see line B). R_i is given by eq 1.

$$R_i = -\mathrm{d[TEMPO]}/\mathrm{d}t = [\mathrm{TEMPO}]_0/\text{induction period} \quad (1)$$

Then, R_i^B is 0.97×10^{-5} mol/(L s) from the slope for the initiator AADC system. Similar experiments were also carried out using model compound DCIA as the initiator. The relationship of induction periods and feed of TEMPO for initiator DCIA system is also shown in Figure 6 (line A; feed conditions: [EMA] = 3.9 mol/L, [DCIA] = 6.33×10^{-2} mol/L, [TEMPO] = 0.016, 0.04, and 0.08 mol/L). R_i^A was determined to be 2.07×10^{-5} mol/(L s) from the slope for the initiator DCIA system.

On the other hand, R_i is given as the following equation from the initiation kinetic:

$$R_i = k_d f[\mathrm{I}] \quad (2)$$

where k_d, f, and [I] are the disproportionation rate constant, initiator efficiency, and initiator concentration, respectively. Under the assumption that f is equal to unity, k_d^A and k_d^B were determined to be 3.27×10^{-4} and 1.38×10^{-4} s^{-1}, respectively. So, the reciprocal of these first-order rate constants means the lifetime of both model DCIA and AADC radicals induced by UV irradiation.

Observed trends for k_d^A and k_d^B can be discussed by C−S bond dissociation energies for model compounds predicted from density functional theory calculations. Figure 7 shows the results of C−S bond dissociation energies and bond lengths for several model compounds. Steric factors are important in determining the bond dissociation energies. This should be reflected in longer lengths for the breaking C−S bond in the ground state for which steric factors are greated. The calculations predict that the values of C−S bond lengths increase in the order DCIA > AADC = **1**; i.e., formation of the tertiary isobutyric acid ester radical should predominate over that of the primary ethyl ester-type radical. Moad et al.[15] and Kazmaier et al.[23] reported the molecular orbital calculations of alkoxyamine homolysis rates on alkoxyamine-initiated living radical polymerization. Prediction showed a marked dependence on the structure of both the nitroxide and radical compounds. In the case of secondary and tertiary alkoxyamines, steric factors appeared to be the dominant influence. The bond dissociation tendency obtained in our work is very similar to their results. However, the C−S bond dissociation energies of dimer **2** have different trends

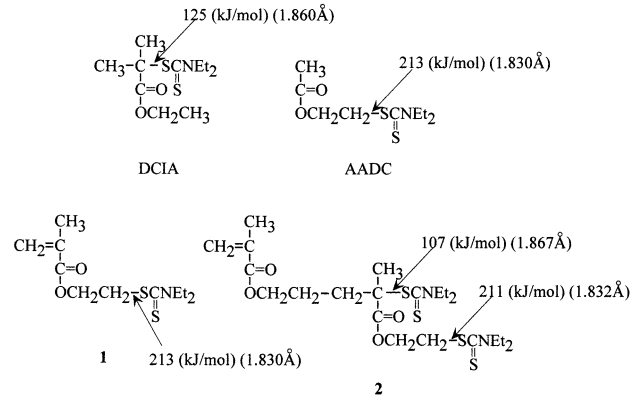

Figure 7. Results of C−S bond dissociation energies and bond lengths for several model compounds calculated assuming a homolytic bond cleavage at B3L YP/6-31G(d) corrected with zero-point energy.

(Figure 7). The dimer **2** has two DC active sites. The C−S bond dissociation energy at the A* group is extremely small (107 kJ/mol). Therefore, the propagation rate from A* position should be faster than that from B* position. It was mentioned earlier that the intercept in Figure 4 (M_n vs conversion) corresponded to the M_n of an 48-mer. This effect seems to reflect the experimental results that the additions occurred faster in the initial stage of hyperbranched polymer formation.

Subsequently, we estimated the propagation rate R_p^A using model compound DCIA. Photopolymerizations of EMA ($[EMA]_0 = 3.9$ mol/L) were carried out in benzene at 40 °C initiated by DCIA ($[DCIA]_0 = 6.33 \times 10^{-2}$ mol/L), varying the irradiation time. The first-order time−conversion plot in the photopolymerization is shown in Figure 3. Straight line in the semilogarithmic coordinates indicates a constant concentration of the active polymer radical P_A*. The slope of the semilogarithmic plot, $S_A = k_p^A[P_A^*]$, was set equal to 1.30×10^{-4} s^{-1}. This value corresponds to pseudo-first-order rate constant. Then, the lifetime of model DCIA radical ($k_d^A = 3.27 \times 10^{-4}$ s^{-1}) becomes shorter (ca. 2.5-fold) compared to that of active polymer radical P_A*; i.e., the primary radical is more active than the PEMA radical P_A*. These results fit well to general information for radical reactivities. We can obtain the absolute rate constant, k_p^A, when the radical concentration [P_A*] is known value. We could not accurately determine [P_A*] by electron spin resonance (ESR) under UV irradiation due to weak ESR signals. In this work, the propagation rate constant k_p for EMA was calculated with the established relation[24] as follows:

$$k_p \text{ (L/(mol s))} = 1.50 \times 10^6 \exp[-20.46 \text{ (kJ/mol)}/RT] \quad (3)$$

where R and T are the gas constant and absolute temperature, respectively. The value of k_p was calculated to be 577.5 L/(mol s). Figure 8 shows the plot of PEMA radical concentration [P_A*] vs time, estimated from the slope of the first-order plot (line A in Figure 3). The open circles and the straight line indicate the estimated values and [P_A*] in the steady state, respectively. As a result, the value of the radical concentration [P_A*] could be estimated to be 3.0×10^{-7} mol/L.

As mentioned earlier, photopolymerization of inimer **1** proceeded with competitive living radical mechanisms between the active A* and B* groups. So, the propagation rate constant k_p^B can be estimated logically from the slope of line H shown in Figure 3, when radical concentrations [P_A*] and [P_B*] are known values for the formation system of hyperbranched polymers. However, the assignment of active species P_A* and P_B* could not be distinguished even by using ESR spectra. In the reaction elements shown in Scheme 1, one can see that k_p^B corresponds to the rate constant reacting of the initiating B* groups to vinyl group of any other molecule. Then, this rate can be regarded as the initiation rate R_i^B.

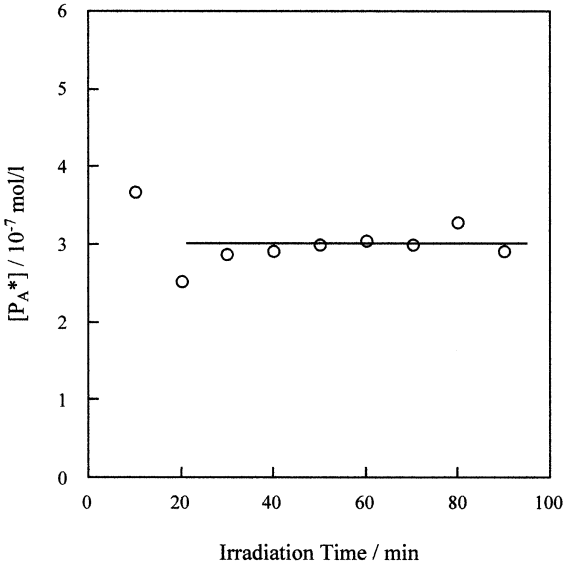

Figure 8. Plot of PEMA radical concentration [P_A*] vs time, estimated from the slope of the first-order plot (line A in Figure 3) by assuming $k_p = 577.5$ L/(mol s): open circles and straight line indicate the estimated values and [P_A*] in the steady state, respectively.

Table 2. Calculated DB_∞ as a Parameter

	reactivity ratio	
	$r = S_A/k_d^B$	$r = k_d^A/k_d^B$
r	0.94	2.37
DB_∞	0.46	0.50

Next, we discuss the degree of branching (DB) of hyperbranched molecules using the reaction rates (the first-order rate constants: k_d^A, k_d^B, and $k_p^A[P_A^*]$) obtained in this work. Müller and co-workers[16,25] have calculated the DB of hyperbranched polymers made by self-condensing vinyl polymerization from kinetic considerations. They obtained the relationship between the DB for full conversion (DB_∞) and reactivity ratio $r = k_p^A/k_p^B$. Such calculations assume that the rate constants for propagation of both inimer and monomer do not change with conversion, and no additional reactions occur. In this case the polydispersity index of the polymer is very high and sharply increases with conversion. As can be seen from Figure 4, the evolution of M_n and M_w/M_n with conversion is absolutely different than that predicted in refs 16 and 25. Although this problem has been left unsolved, we estimated the DB_∞ as a parameter of reactivity ratios using the first-order rate constants (see Table 2). The DB_∞ shows ca. 0.5 in the range of $r = 0.94-2.37$. The DB can be regarded as the ratio of branched units in the polymer to those in a perfect dendrimer. The limiting values are DB = 0 for linear polymers and DB = 1 for a perfect dendrimer. The statistical process of forming hyperbranched gives

DB ≤ 0.5.[25,26] The hyperbranched molecules formed from controlled radical process of inimer **1** are not perfect dendritic but somewhat defect structures. It is difficult to determine the DB by NMR spectroscopy because the proton signals of branch points (ethylene protons: −C(=O)−O−CH_2CH_2−) overlap with proton signals of the main chains.

As mentioned earlier, some other parameters could be useful to prove branched structure. In the previous paper,[13] we made clear the compact nature of hyperbranched PEMA. That is, branching factor g' (= $[\eta]/[\eta]_L$) decreased with increasing M_w, where $[\eta]$ and $[\eta]_L$ are intrinsic viscosities of hyperbranched polymer and the linear polymer molecule with identical molecular mass. The ratio R_g/R_h (R_g = radius of gyration, R_h = hydrodynamic radius) is a sensitive fingerprint of the inner density profile of star molecules and polymer micelles. The values of R_g/R_h for the hyperbranched PEMA (M_w = 17.0 × 10^4−4.4 × 10^4) were in the range 0.75−0.84 in a good solvent. It is well-known that the R_g/R_h value for hard spheres of uniform density is 0.775.[27,28] The hyperbranched molecules possessing high M_w behaved almost as hard spheres in a good solvent. Therefore, the DB obtained in this work seems reasonable. Kinetic analysis is one of the best methods to determine the DB of hyperbranched molecules. Unfortunately, clear-cut evidence for the branched structure in the initial stage and low polydispersity index as compared with theoretical prediction was not obtained in this work.

Conclusions

We studied the living nature on the formation of hyperbranched poly(methacrylic acid ester) by free radical photopolymerization of inimer DTEM. From the first-order time−conversion plots, this polymerization system proceeded with the competitive living radical mechanisms between the initiator radical B* and the monomer vinyl radical A*. We analyzed the initiation step using model compounds AADC and DCIA with an aid of TEMPO as radical scavenger. As a result, the disproportionation rate constants k_d^A and k_d^B were estimated to be 3.27 × 10^{-4} and 1.38 × 10^{-4} s^{-1}, respectively. We also analyzed the propagation step from photopolymerization of EMA initiated by model compound DCIA. The polymerization of EMA also proceeded with controlled radical mechanism. The pseudo-first-order rate constant $k_p^A[P_A^*]$ was calculated to be 1.30 × 10^{-4} s^{-1}. The lifetime of primary DCIA radical became shorter compared to that of active polymer radical P_A^*. The DB for full conversion (DB_∞) was calculated to be ca. 0.5 using Müller's theoretical equation concerning the reactivity ratios. The hyperbranched molecules formed by controlled radical process of inimer DTEM are not perfect dendritic but somewhat defect structures.

Acknowledgment. This work was supported in part by a Grant-in-Aid for Scientific Research, No. 13650927, from the Ministry of Education, Science, Sports and Culture, Japan. The density functional theory calculations were carried out at the computer center of the Tokyo Institute of Technology and the computer center of the Institute for Molecular Science, and we thank them for their generous permission to use the SG1 Origin2000 and Compaq Alpha Server GS320 and IBM SP2, respectively.

References and Notes

(1) Mishra, M. K., Kobayashi, S., Eds. In *Star and Hyperbranched Polymers*; Polymer Frontiers International: New York, 1995.
(2) Ishizu, K.; Tsubaki, K.; Mori, A.; Uchida, S. *Prog. Polym. Sci.* **2003**, *28*, 27.
(3) Fréchet, J. M. J.; Henmi, M.; Gitsov, I.; Aoshima, S.; Leduc, M. R.; Grubbs, R. B. *Science* **1995**, *269*, 1080.
(4) Hawker, C. J.; Fréchet, J. M. J.; Grubbs, R. B.; Dao, J. *J. Am. Chem. Soc.* **1995**, *117*, 10763.
(5) Fréchet, J. M. J.; Aoshima, S. US Patent 5 587 441, 1996.
(6) Fréchet, J. M. J.; Aoshima, S. US Patent 5 587 446, 1996.
(7) Gaynor, S. G.; Edelman, S.; Matyjaszewski, K. *Macromolecules* **1996**, *29*, 1079.
(8) Weimer, M. W.; Fréchet, J. M. J.; Gitsov, I. *J. Polym. Sci., Polym. Chem. Ed.* **1998**, *36*, 955.
(9) Li, C.; He, J.; Li, L.; Cao, J.; Yang, Y. *Macromolecules* **1999**, *32*, 7012.
(10) Tao, Y.; He, J.; Wang, Z.; Pan, J.; Jiang, H.; Chen, S.; Yang, Y. *Macromolecules* **2001**, *34*, 4742.
(11) Niu, A.; Li, C.; Zhao, Y.; He, J.; Yang, Y.; Wu, C. *Macromolecules* **2001**, *34*, 460.
(12) Ishizu, K.; Mori, A. *Macromol. Chem. Rapid Commun.* **2000**, *21*, 665.
(13) Ishizu, K.; Shibuya, T.; Mori, A. *Polym. Int.* **2002**, *51*, 424.
(14) Ishizu, K.; Mori, A. *Polym. Int.* **2001**, *50*, 906.
(15) Moad, G.; Rizzardo, E. *Macromolecules* **1995**, *28*, 8722.
(16) Müller, A. H. E.; Yan, D.; Wulkov, M. *Macromolecules* **1997**, *30*, 7015.
(17) Ishizu, K.; Ohta, Y.; Kawauchi, S. *Macromolecules* **2002**, *35*, 3781.
(18) Otsu, T.; Yoshida, M. *Makromol. Chem. Rapid Commun.* **1982**, *3*, 127.
(19) Otsu, T.; Kuriyama, A. *J. Macromol. Sci., Chem.* **1984**, *A21*, 961.
(20) Otsu, T.; Yamashita, K.; Tsuda, K. *Macromolecules* **1986**, *19*, 287.
(21) Brandrup, J., Immergut, E. H., Grulke, E. A., Eds. In *Polymer Handbook*, 4th ed.; John Wiley & Sons: New York, 1999.
(22) Frisch, M. J.; Trucks, G. W.; Schlegel, H. B.; Scuseria, G. E.; Robb, M. A.; Cheeseman, J. R.; Zakrzewski, V. G.; Montgomery, J. A., Jr.; Stratmann, R. E.; Burant, J. C.; Dapprich, S.; Millam, J. M.; Daniels, A. D.; Kodin, K. N.; Strain, M. C.; Farkas, O.; Ochterski, J.; Petersson, G. A.; Ayala, P. Y.; Cui, Q.; Morokuma, K.; Malick, D. K.; Rabuck, A. D.; Raghavachari, K.; Foreman, J. B.; Cioslowski, J.; Ortize, J. V.; Baboul, A. G.; Stefanov, B. B.; Liu, G.; Liashenko, A.; Piskorz, P.; Komaromi, I.; Gomperts, R.; Martin, R. L.; Fox, D. J.; Keith, T.; Al-Laham, M. A.; Peng, C. Y.; Nanayakkara, A.; Gonzalez, C.; Head-Gordon, M.; Replogle, E. S.; Pople, J. A. *Gaussian 98*, revision A.7; Gaussian, Inc.: Pittsburgh, PA, 1998.
(23) Kazmaier, P. M.; Moffat, K. A.; Georges, M. K.; Veregin, R. P. N.; Hamer, G. K. *Macromolecules* **1995**, *28*, 1841.
(24) Davis, T. P.; O'Driscoll, K. F.; Piton, M. C.; Winnik, M. A. *Macromolecules* **1990**, *23*, 2113.
(25) Yan, D.; Müller, A. H. E.; Matyjaszewski, K. *Macromolecules* **1997**, *30*, 7024.
(26) Hölter, D.; Burgath, A.; Frey, H. *Acta Polym.* **1997**, *48*, 30.
(27) Yamakawa, H. In *Modern Theory on Polymer Solution*; Harper & Row: New York, 1971; p 321.
(28) Antonietti, M.; Bremser, W.; Schmidt, M. *Macromolecules* **1990**, *23*, 3796.

MA021729Q